Zerumbone Abolishes RANKL-Induced NF-κB Activation, Inhibits Osteoclastogenesis, and Suppresses Human Breast Cancer–Induced Bone Loss in Athymic Nude Mice

Bokyung Sung,[1] Akira Murakami,[2] Babatunde O. Oyajobi,[3] and Bharat B. Aggarwal[1]

[1]Cytokine Research Laboratory, Department of Experimental Therapeutics, The University of Texas M. D. Anderson Cancer Center, Houston, Texas; [2]Division of Food Science and Biotechnology, Graduate School of Agriculture, Kyoto University, Kyoto, Japan; and [3]Department of Cellular and Structural Biology, The University of Texas Health Science Center at San Antonio, San Antonio, Texas

Abstract

Receptor activator of nuclear factor-κB (NF-κB) ligand (RANKL) has emerged as a major mediator of bone resorption, commonly associated with cancer and other chronic inflammatory diseases. Inhibitors of RANKL signaling thus have potential in preventing bone loss. In the present report, the potential of zerumbone, a sesquiterpene derived from subtropical ginger, to modulate osteoclastogenesis induced by RANKL and breast cancer was examined. We found that zerumbone inhibited RANKL-induced NF-κB activation in mouse monocyte, an osteoclast precursor cell, through inhibition of activation of IκBα kinase, IκBα phosphorylation, and IκBα degradation. Zerumbone also suppressed RANKL-induced differentiation of these cells to osteoclasts. This sesquiterpene also inhibited the osteoclast formation induced by human breast tumor cells and by multiple myeloma cells. Finally, we examined whether zerumbone could prevent human breast cancer–induced bone loss in animals. We found that zerumbone decreased osteolysis in a dose-dependent manner in MDA-MB-231 breast cancer tumor-bearing athymic nude mice. These results indicate that zerumbone is an effective blocker of RANKL-induced NF-κB activation and of osteoclastogenesis induced by RANKL and tumor cells, suggesting its potential as a therapeutic agent for osteoporosis and cancer-associated bone loss. [Cancer Res 2009;69(4):1477–84]

Introduction

Bone remodeling is controlled by the balance between bone formation and resorption (1). Many bone-related diseases, such as osteoporosis, rheumatoid arthritis, Paget's disease, and cancer-induced osteolysis, are characterized by excessive bone resorption by osteoclast, multinucleated cells derived from hematopoietic cells (1). The differentiation of osteoclast precursors to osteoclast is regulated by the bone microenvironment, which includes stromal cells, osteoblasts, and other local factors (2). Perhaps two most proteins crucial for osteoclast differentiation and activation are receptor activator of nuclear factor-κB (NF-κB; RANK) and its ligand, RANKL. The latter is a member of the tumor necrosis factor (TNF) superfamily of cytokines (3), and its expression is regulated by several factors that regulate bone resorption, including vitamin D3, glucocorticoids, interleukin (IL)-1, IL-6, and TNFα (2, 4, 5). The significance of RANK-RANKL pathway is supported by studies that show that disruption in either *rank* or *rankl* in mice produced severe osteopetrosis and defective tooth eruption resulting from a complete lack of osteoclasts (6). In contrast, genetic deletion of osteoprotegerin, a decoy receptor for RANKL and an inhibitor of RANK, produced osteoporosis resulting from an increased number of osteoclast (7).

Bone metastases represent a common cause of morbidity in patients with many types of cancer, occurring in up to 70% of patients with advanced breast or prostate cancer and in about 15% to 30% of patients with lung, colon, kidney, thyroid, and stomach carcinoma (8). Bone metastases can cause hypercalcemia, bone fragility, pathologic fractures, and spinal compression and are usually associated with severe bone pain due to osteolysis, which can be intractable (9). Besides solid tumors, osteolysis is present in other pathologies, such as psoriatic arthritis, periodontal disease, and multiple myeloma (10–12).

Above description thus indicates that agents that can suppress RANKL signaling have potential for treatment of osteoporosis. In the present report, we investigated whether zerumbone, a sesquiterpene derived from tropical ginger *Zingiber zerumbet*, can modulate RANKL-induced signaling and osteoclastogenesis. Zerumbone has been shown to suppress azoxymethane-induced rat aberrant crypt foci (13), inhibit dextran sodium sulfate–induced colitis in mice (14), suppress skin tumor initiation and promotion in mice (15), inhibit tumor growth in mice (16), and reduce cholecystokinin-induced pancreatitis in rats (17). Previously, we have shown that this agent can down-regulate NF-κB activation induced by various carcinogens and inflammatory agents and suppress NF-κB–regulated gene products (18). The current report is based on the hypothesis that zerumbone would also suppress RANKL signaling and RANKL-induced osteoclastogenesis. We found that zerumbone can suppress RANKL-induced NF-κB activation through inhibition of IκBα kinase (IKK) and inhibits osteoclastogenesis induced by RANKL and by breast cancer and multiple myeloma cells.

Materials and Methods

Reagents. Zerumbone (Fig. 1*A*), isolated as described (19), was prepared as a 50 mmol/L solution in DMSO and then further diluted in cell culture medium. DMEM/F12, RPMI 1640, DMEM, fetal bovine serum, 0.4% trypan blue vital stain, and antibiotic-antimycotic mixture were obtained from Invitrogen. Rabbit polyclonal antibodies to IκBα were purchased from Santa Cruz Biotechnology. Antibody against phospho-IκBα ($Ser^{32/36}$) was purchased from Cell Signaling Technology. Anti-IKKα and anti-IKKβ antibodies were kindly provided by Imgenex. Goat anti-rabbit and goat

Note: Supplementary data for this article are available at Cancer Research Online (http://cancerres.aacrjournals.org/).

Requests for reprints: Bharat B. Aggarwal, Cytokine Research Laboratory, Department of Experimental Therapeutics, The University of Texas M. D. Anderson Cancer Center, 1515 Holcombe Boulevard, Box 143, Houston, TX 77030. Phone: 713-794-1817; Fax: 713-745-6339; E-mail: aggarwal@mdanderson.org.

doi:10.1158/0008-5472.CAN-08-3249

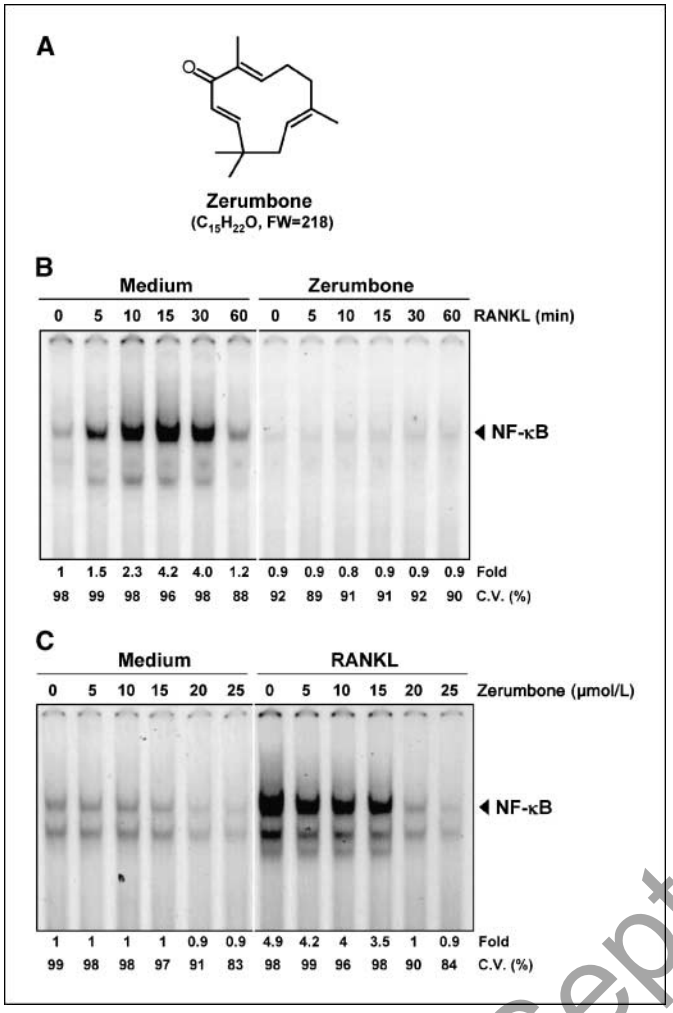

Figure 1. RANKL induces NF-κB activation and zerumbone inhibits it in a dose-dependent and time-dependent manner. *A,* structure of zerumbone. *B,* RAW 264.7 cells (1×10^6) were incubated with zerumbone (20 μmol/L) for 12 h, treated with 10 nmol/L RANKL for the indicated times, and assayed for NF-κB activation by electrophoretic mobility shift assay. *C,* RAW 264.7 cells (1×10^6) were incubated with or without the indicated concentrations of zerumbone and RANKL (10 nmol/L) and tested for NF-κB activation by electrophoretic mobility shift assay. Fold value is based on the value for medium (control), arbitrarily set at 1. The cell viability (*C.V.*) was determined by the trypan blue exclusion assay.

anti-mouse horseradish peroxidase conjugates were purchased from Bio-Rad. Antibody against β-actin and leukocyte acid phosphatase kit (387-A) for tartrate-resistant acid phosphatase (TRAP) staining were purchased from Sigma-Aldrich. Protein A/G-agarose beads were obtained from Pierce. [γ-^{32}P]ATP was purchased from ICN Pharmaceuticals.

Cell lines. RAW 264.7 (mouse macrophage), MDA-MB-231 (human breast adenocarcinoma), and U266 cells (human multiple myeloma) were obtained from the American Type Culture Collection. RAW 264.7 cells were cultured in DMEM/F12 supplemented with 10% fetal bovine serum and antibiotics. This cell line is a well-established osteoclastogenic cell system that has been shown to express RANK and differentiate into functional TRAP-positive osteoclasts when cultured with soluble RANKL (20). Moreover, RANKL has been shown to activate NF-κB in RAW 264.7 cells (21). MDA-MB-231 cells in DMEM and U266 cells were cultured in RPMI 1640 with 10% fetal bovine serum.

Electrophoretic mobility shift assays for NF-κB. Nuclear extracts were prepared as described previously (22). Briefly, nuclear extracts from RANKL-treated cells were incubated with ^{32}P-end-labeled 45-mer double-stranded NF-κB oligonucleotide (15 μg protein with 16 fmol DNA) from the HIV long terminal repeat, 5′-TTGTTACAA**GGGACTTTC**CGCTG**GGGACTTTC**CAGG-GGGAGGCGTGG-3′ (boldface indicates NF-κB–binding sites), for 30 min at 37°C, and the DNA-protein complex formed was separated from free oligonucleotide on 6.6% native polyacrylamide gels. The dried gels were visualized with a Storm820 and radioactive bands were quantified using ImageQuant software (Amersham).

Western blot analysis. To determine the levels of protein expression in the cytoplasm or nucleus, we prepared extracts (22) and fractionated them by 10% SDS-PAGE. After electrophoresis, the proteins were electro-transferred to nitrocellulose membranes, blotted with each antibody, and detected by enhanced chemiluminescence reagent (GE Healthcare).

Reverse transcription-PCR analysis. RANKL mRNA expression was determined by reverse transcription-PCR (RT-PCR). MDA-MB-231 cells were treated with zerumbone for 24 h. Total RNA was extracted from cells using Trizol (Invitrogen). One microgram of total RNA was converted to cDNA by SuperScript reverse transcriptase and then amplified by Platinum Taq polymerase using SuperScript One-Step RT-PCR kit (Invitrogen). The primers include those for RANKL (forward primer, 5′-CGTTGGATCACAG-CACATCAG-3′; reverse primer, 5′-AGTATGTTGCATCCTGATCCG-3′) and glyceraldehyde-3-phosphate dehydrogenase (GAPDH; forward primer, 5′-GTCTTCACCACCATGGAG-3′; reverse primer, 5′-CCACCCTGTTGCTG-TAGC-3′). Cycling conditions were 30-s denaturation at 94°C, 30-s annealing at 56°C, and 30-s elongation at 72°C for 35 cycles. PCR products were electrophoresed on 2% agarose gels and gel images were visualized under UV light and photographed.

Trypan blue exclusion assay. Cells were harvested from the 24-well plates by treatment with 0.2% trypsin-EDTA, centrifuged, and suspended with 1 mL culture medium. Cell suspension was mixed with equal volume of 0.4% isotonic trypan blue solution. Total cell number and fraction of nonviable, dye-accumulating cells were counted after 2 min in Fuchs-Rosenthal hemocytometer under light microscope.

IKK assay. To determine the effect of zerumbone on RANKL-induced IKK activation, IKK assay was done by a method described previously (22). Briefly, the IKK complex from whole-cell extracts (800 μg protein) was precipitated with antibody against IKKα followed by treatment with protein A/G-agarose beads. After 2 h of incubation, the beads were washed with lysis buffer and assayed in a kinase assay mixture containing 50 mmol/L HEPES (pH 7.4), 20 mmol/L $MgCl_2$, 2 mmol/L DTT, 20 mCi [γ-^{32}P]ATP, 10 mmol/L unlabeled ATP, and 2 μg substrate glutathione *S*-transferase (GST)-IκBα (amino acids 1–54). After incubation at 30°C for 30 min, the reaction was terminated by boiling with SDS sample buffer for 5 min. Finally, the protein was resolved on 10% SDS-PAGE, the gel was dried, and the radioactive bands were visualized with a PhosphorImager. To determine the total amounts of IKKα and IKKβ in each sample, the whole-cell protein was resolved on 10% SDS-PAGE, electrotransferred to a nitrocellulose membrane, and blotted with anti-IKKα or anti-IKKβ antibody.

Osteoclast differentiation assay. RAW 264.7 cells were cultured in 24-well dishes at a density of 5×10^3 per well and allowed to adhere overnight. The medium was then replaced, and the cells were treated with 5 nmol/L RANKL for 5 d. All cell lines were subjected to TRAP staining using leukocyte acid phosphatase kit (387-A).

***In vivo* osteolytic bone metastasis assay.** The estrogen-independent human breast cancer cell line MDA-MB-231 was cultured and resuspended in PBS to give a final concentration of 1×10^5/100 μL, which was injected directly into the left ventricle of 4- to 5-wk-old female BALB/c *nu/nu* mice (Harlan) via a percutaneous approach. The mice were then randomly assigned to one of three groups ($n \geq 9$/group), treated with vehicle (0.9% sodium chloride) or zerumbone (20 or 100 mg/kg body weight in vehicle) by i.p. injection three times a week for 28 d, and then sacrificed. Radiographs (Faxitron radiographic inspection unit, Kodak) were obtained at baseline and just before sacrifice. Area of osteolytic bone metastases on X-rays of tibiae and femorae, recognized as well-circumscribed radiolucent lesions on radiographs, was quantitated using MetaMorph imaging software (Molecular Devices). Radiographs were analyzed by investigators blinded to the composition of the groups in the experiment or the experimental protocol and areal data for each group are presented as mm^2/lesion (mean ± SE).

Immunohistochemistry. Bone histology and histomorphometric analysis of bone tissue sections were performed as previously described with minor modifications (23). Briefly, on day 28 after tumor cell inoculation, animals treated with vehicle or zerumbone were sacrificed; both hind limbs from each animal were harvested, fixed in 10% formalin, decalcified in EDTA, and embedded in paraffin; and 4- to 5-μm-thick sections of undecalcified long bones were cut with a Leica microtome. Sections were stained with H&E, orange G, and phloxine. Histomorphometric analysis for tumor burden was performed on H&E-stained sections of tibiae using the MetaMorph computerized image analysis system. Tumor burden is expressed as a percentage of the total area of medullary cavity (between the cortices and a fixed distance from the growth plate) that is occupied by tumor. Osteoclasts were detected *in situ* in serial sections as previously described by cytochemical staining for TRAP activity, a marker of osteoclasts (23).

Statistical analysis. Data are presented as mean ± SE and analyzed using StatView software (version 5.0; SAS Institute, Inc.). Statistical significance of differences was assessed using the nonparametric Mann-Whitney *U* test. Values of $P \leq 0.05$ were considered statistically significant.

Results

The aim of the present study was to investigate the effect of zerumbone on RANKL signaling that leads to osteoclastogenesis. Whether zerumbone could modulate osteoclastogenesis induced by tumor cells was another focus of these studies. We used the RAW 264.7 cell (murine macrophage) system, as it is a well-established model for osteoclastogenesis (24).

Zerumbone abrogates RANKL-induced NF-κB activation. To investigate whether zerumbone modulates RANKL-induced NF-κB activation in RAW 264.7 cells, cells were either pretreated with zerumbone for 12 hours or left untreated and then exposed to RANKL for indicated times, nuclear extracts were prepared, and NF-κB activation was assayed by electrophoretic mobility shift assay. As shown in Fig. 1*B*, RANKL activated NF-κB in a time-dependent manner; however, zerumbone completely abrogated RANKL-induced NF-κB activation (Fig. 1*B*).

To determine the minimum concentration of zerumbone required to suppress RANKL-induced NF-κB activation, cells were pretreated with various concentrations of zerumbone and then exposed to RANKL. Zerumbone almost completely suppressed NF-κB activation at 20 μmol/L (Fig. 1*C*). Treatment of cells with 20 μmol/L zerumbone for 12 hours had no effect on cell viability as determined by the trypan blue exclusion method.

Zerumbone inhibits RANKL-induced IκBα phosphorylation and degradation. Most cytokines activate NF-κB through phosphorylation and degradation of its inhibitory subunit IκBα (25). To identify the mechanism involved in the inhibition of NF-κB activation by zerumbone, we first checked the effect on zerumbone on level of IκBα by using Western blot analysis. In cells treated with RANKL, the IκBα level dropped within 5 minutes and returned to normal level within 60 minutes (Fig. 2*A, left*). In contrast, cells pretreated with zerumbone showed suppressed RANKL-induced degradation of IκBα (Fig. 2*A, right*).

Next, we investigated the effect of zerumbone on the phosphorylation of IκBα, which occurs before its ubiquitination and degradation (25). We used the proteasome inhibitor *N*-acetyl-leu-leu-norleucinal (ALLN) to prevent RANKL-induced IκBα degradation. Western blot analysis for phospho-IκBα in Fig. 2*B* clearly indicates that RANKL induced IκBα phosphorylation in RAW 264.7 cells and that zerumbone abrogated this effect. Zerumbone alone did not result in phosphorylation of IκBα.

Zerumbone inhibits RANKL-induced IKK activation. Because zerumbone inhibits the phosphorylation and degradation of IκBα, we next checked whether zerumbone alters the activity or the levels of IKK, which leads to IκBα phosphorylation. Immunocomplex kinase assay on cells treated with RANKL showed a sharp increase in IKK activity as indicated by the phosphorylation of GST-IκBα within 3 minutes. In contrast, cells pretreated with zerumbone could not phosphorylate GST-IκBα on RANKL treatment (Fig. 2*C, top*). To check whether the apparent loss of IKK activity was due to the loss of IKK protein expression, the levels of the IKK subunits IKKα and IKKβ were tested by Western blot analysis. Results in Fig. 2*C* clearly show that zerumbone treatment did not alter the expression of IKKα and IKKβ.

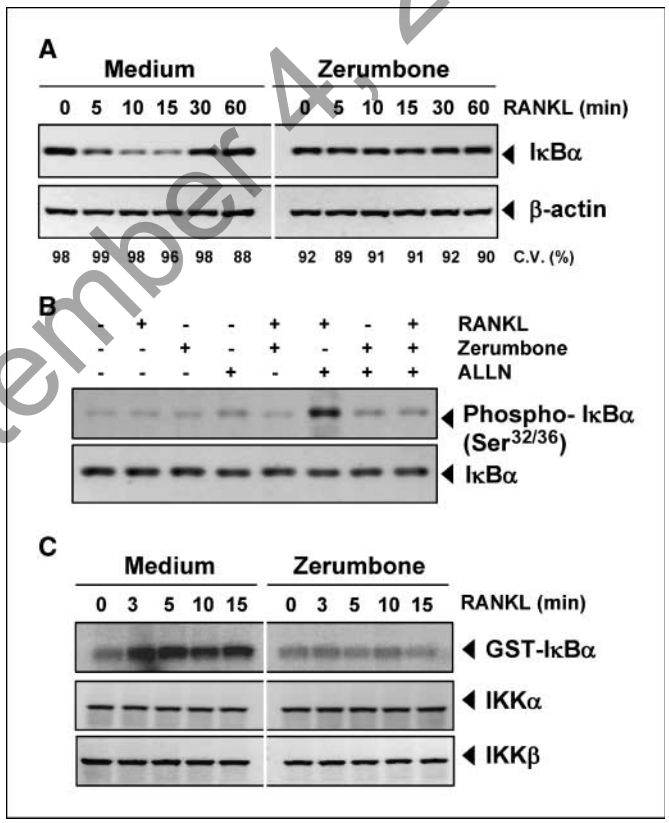

Figure 2. Zerumbone suppresses RANKL-induced IκBα degradation (*A*) and phosphorylation (*B*) through inhibition of IKK activity (*C*). *A,* RAW 264.7 cells (1×10^6) were incubated with zerumbone (20 μmol/L) for 12 h and then treated with RANKL (10 nmol/L) for the indicated times. Cytoplasmic extracts were prepared, fractionated by 10% SDS-PAGE, and electrotransferred to nitrocellulose membranes. Western blot analysis was performed with anti-IκBα. The cell viability was determined by the trypan blue exclusion assay. *B,* RAW 264.7 cells (1×10^6) were pretreated with zerumbone (20 μmol/L) for 12 h, then incubated with ALLN (50 μg/mL for 30 min), and then treated with RANKL (10 nmol/L) for 15 min. Cytoplasmic extracts were prepared, fractionated by 10% SDS-PAGE, and electrotransferred to nitrocellulose membranes. Western blot analysis was performed using either anti-phospho-IκBα (*top*) or anti-IκBα (*bottom*). *C,* RAW 264.7 cells (3×10^6) were pretreated with zerumbone (20 μmol/L) for 12 h, incubated with 50 μg/mL ALLN for 30 min, and then incubated with RANKL (10 nmol/L) for the indicated times. Whole-cell extracts were immunoprecipitated using antibody against IKKα and analyzed by an immune complex kinase assay using recombinant GST-IκBα as described in Materials and Methods. To examine the effect of zerumbone on the level of IKK proteins, whole-cell extracts were fractionated by 10% SDS-PAGE and examined by Western blot analysis using anti-IKKα (*middle*) and anti-IKKβ (*bottom*) antibodies.

Zerumbone inhibits RANKL-induced osteoclastogenesis. Next, the effect of zerumbone on RANKL-induced osteoclastogenesis was examined. RAW 264.7 cells were incubated with different concentrations of zerumbone in the presence of RANKL and allowed to differentiate into osteoclasts. As shown in Fig. 3*A*, RANKL induced osteoclasts in the absence of zerumbone at day 4. By contrast, the differentiation into osteoclast was significantly decreased in the presence of zerumbone. In addition, the formation of osteoclast decreased with increasing concentration of zerumbone (Fig. 3*B*). As little as 0.5 μmol/L zerumbone had a significant effect on RANKL-induced osteoclast formation. Under these conditions, the viability of cells was not significantly affected (Supplementary Fig. S1).

Zerumbone acts at an early step in the pathway leading to RANKL-induced osteoclastogenesis. It normally takes up to 5 days for RAW 264.7 cells to differentiate into osteoclasts in response to RANKL. To elucidate how early zerumbone acts in this pathway, RAW 264.7 cells were treated initially with RANKL, zerumbone was added 1, 2, 3, and 4 days after RANKL addition, and then its effect on osteoclast formation was determined. Zerumbone inhibited osteoclastogenesis even when the cells were exposed 24 hours after the RANKL treatment. However, the inhibitory effect decreased significantly in a time-dependent manner when cells were treated with zerumbone after RANKL treatment (Fig. 4).

Zerumbone inhibits osteoclastogenesis induced by tumor cells. Osteoclastogenesis is commonly linked with breast cancer (26) and multiple myeloma (27) through the activation of NF-κB (28). Whether zerumbone also inhibits tumor cell–induced osteoclastogenesis of RAW 264.7 cells was investigated. As shown in Fig. 5*A* and *B*, incubating RAW 264.7 cells with breast cancer MDA-MB-231 cells or multiple myeloma U266 induced osteoclast differentiation, and zerumbone suppressed this differentiation. These results indicate that osteoclastogenesis induced by tumor cells is significantly suppressed by the presence of zerumbone.

Whether human breast cancer or multiple myeloma cells express RANKL was examined by RT-PCR. We found that human multiple myeloma U266 cells do express RANKL but human breast cancer cells (MDA-MB-231) do not (Fig. 5*C*).

Zerumbone decreases osteolysis in MDA-MB-231 breast cancer tumor-bearing mice. To determine the effect of zerumbone on bone loss, we used a xenotransplant mouse model. Human breast cancer cells (MDA-MB-231) were injected directly

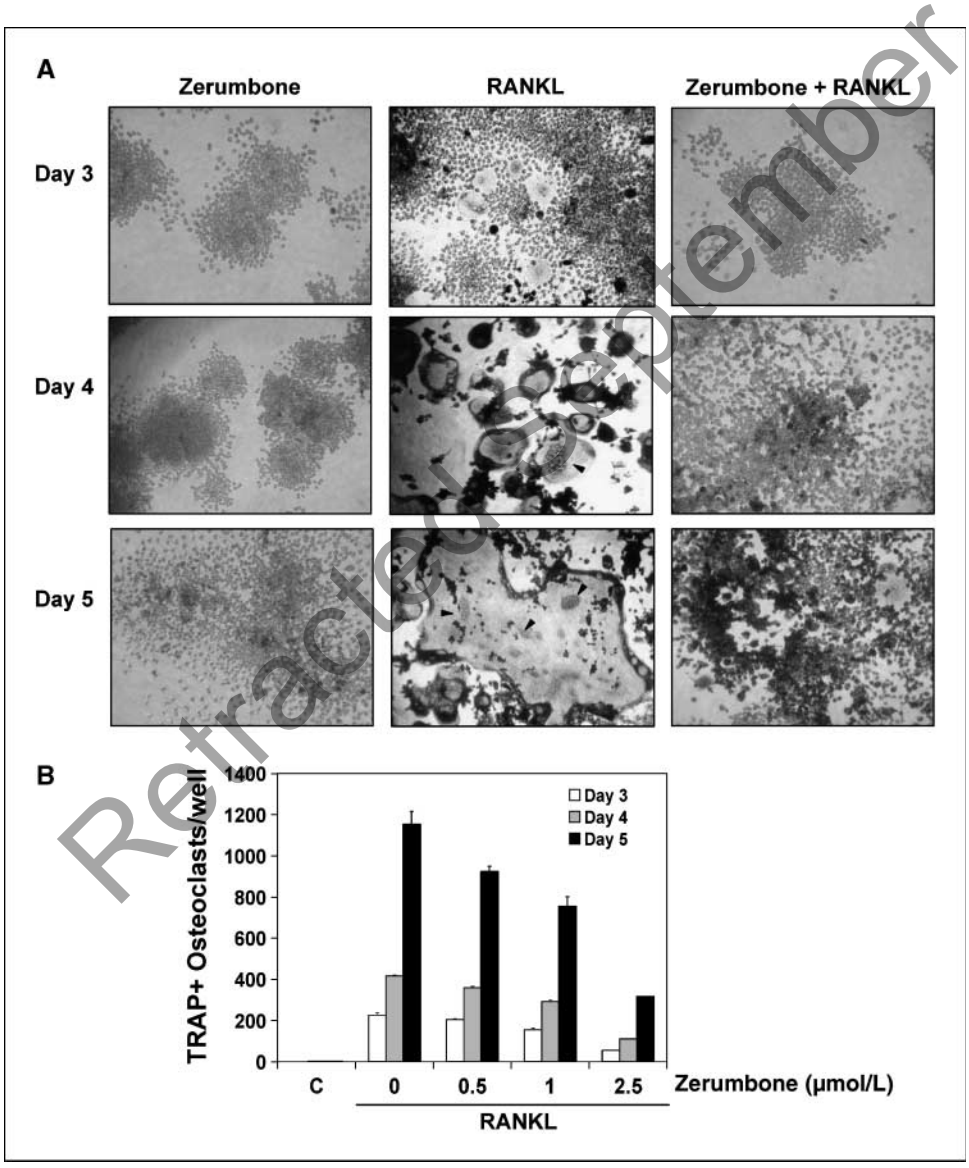

Figure 3. Zerumbone inhibits RANKL-induced osteoclastogenesis. *A,* RAW 264.7 cells (5×10^3) were incubated with either medium or RANKL (5 nmol/L) or RANKL and zerumbone (2 μmol/L) for 3, 4, or 5 d and then stained for TRAP expression. TRAP-positive cells were photographed. *Arrows,* nuclei. Original magnification, ×100. *B,* RAW 264.7 cells (5×10^3) were incubated with either medium or RANKL (5 nmol/L) along with indicated concentration of zerumbone for 3, 4, or 5 d and then stained for TRAP expression. Multinucleated osteoclasts were counted. *C*, cells exposed to medium alone (control).

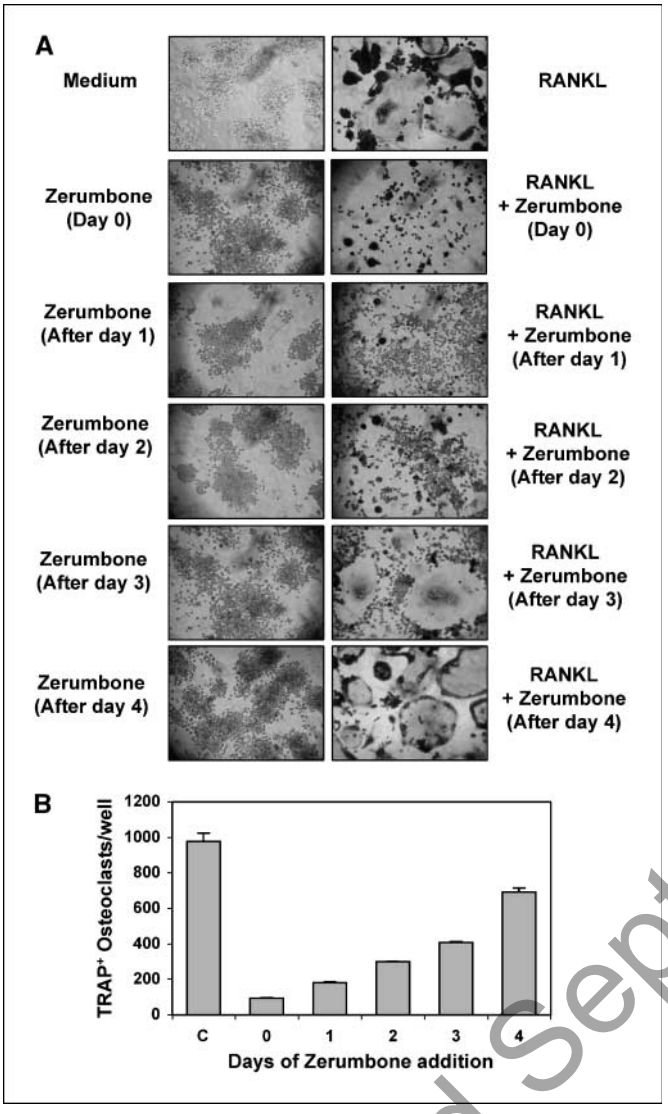

Figure 4. Zerumbone inhibits RANKL-induced osteoclastogenesis 24 h after stimulation. RAW 264.7 cells (5×10^3) were incubated with RANKL (5 nmol/L) and zerumbone (2 μmol/L) for indicated times. *A*, cells were cultured for 5 d after RANKL treatment and stained for TRAP expression. *B*, multinucleated osteoclasts (i.e., those containing three nuclei) were counted. *C*, cells treated with medium alone (control).

into the left ventricle. At day 28, osteolytic bone metastases were detectable by radiography in the majority of the animals in different groups. As shown in Fig. 6*A*, there was no significant difference in body weight between control tumor-bearing mice and zerumbone-administrated groups. This result indicates that zerumbone is nontoxic even at the higher dose (100 mg/kg). The data presented in Fig. 6*B* showed that zerumbone (20 and 100 mg/kg) suppressed osteolytic bone metastases compared with vehicle-treated human breast tumor-bearing mice. The effect was more pronounced at 100 mg/kg than at 20 mg/kg dose of zerumbone. Therefore, as indicated in Fig. 6*C*, human breast cancer induced osteolysis (represented by radiolucency) and the destruction of cortices (*arrows*) in bone of tumor-bearing mice (*left*). In contrast, there was very little osteolysis in bone from the higher dose zerumbone (100 mg/kg)–treated groups and the cortices remained intact (*right*).

Overall tumor burden in tibiae assessed histomorphometrically was statistically not significantly different between the tumor-bearing (Fig. 6*D, a*, 54 ± 9%, $n = 15$) and zerumbone-treated groups (Fig. 6*D, b*, 49 ± 9%, $n = 17$). However, TRAP activity shows intense osteoclast activity with tumor-bearing mice at tumor-bone interface (Fig. 6*D, c*, *pink/red staining*) and also at some distance away from the tumor around the growth plate. In contrast, osteoclast activity is markedly reduced in zerumbone-treated groups (Fig. 6*D, d*). In vehicle-treated tumor-bearing animals, the osteoclasts presented at the tumor-bone interface along the cortico-endosteal surface where they are rarely seen (Fig. 6*D, e*). In contrast, there are no osteoclasts present at the cortico-endosteal surface despite the tumor cells being in contact with bone and the comparable amounts of tumor in the two groups of tumor-bearing animals (Fig. 6*D, f*). These results indicate that zerumbone significantly suppressed the osteolysis in tumor-bearing mice.

Discussion

Bone loss is one of the major problems associated with aging, arthritis, cancer, and other chronic inflammatory illnesses. Identification of inhibitors of bone loss that are safe, efficacious, and affordable is needed. Zerumbone is one such compound that is derived from shampoo ginger and has been shown to suppress inflammatory pathways. The goal of this study was to investigate the effect of zerumbone, a bioactive sesquiterpene, on RANKL-induced NF-κB activation and osteoclastogenesis induced by both RANKL and tumor cells.

Our results indicated that RANKL activated NF-κB in osteoclast precursor cells through the activation of IKK and subsequent IκBα phosphorylation and degradation. The RANKL-induced NF-κB activation signaling pathway differs from that of the TNF-induced pathway. For instance, NIK, which may function as an activator of IKKα, is necessary in RANKL-induced NF-κB activation (21); however, it is dispensable for TNF-induced NF-κB activation (29). Therefore, Novack and colleagues (30) reported that NIK-deficient osteoclast precursors did not respond to RANKL in an *in vitro* differentiation system devoid of osteoblasts. We also found that zerumbone inhibited RANKL-induced IKK activation, leading to the suppression of NF-κB activation.

A recent study established that IKKβ, but not IKKα, is essential for inflammation-induced bone loss and is required for osteoclastogenesis *in vivo* (31). Although the ability of zerumbone to suppress TNF-induced IKK activation has been reported (18), the current study is the first to report that zerumbone can suppress RANKL-induced IKK activation and consequently NF-κB activation. How zerumbone inhibits RANKL-induced IKK activation is not clear. Numerous kinases have been implicated in the activation of IKK, including AKT, mitogen-activated protein kinase (MAPK)/extracellular signal-regulated kinase kinase kinase 1, 2, and 3, glycogen synthase kinase-3β, and NIK (32). Previously, our group has shown that NIK-induced NF-κB activation is blocked by zerumbone (18). Thus, it is possible that zerumbone inhibits RANKL-induced IKK activation through inhibition of NIK. However, other potential mechanisms cannot be ruled out based on the data presented here.

Osteoclastogenesis is dependent on RANKL under physiologic and pathologic conditions (1, 2). Although the mechanism by which RANKL induces osteoclastogenesis is not completely understood, it is known that RANKL-induced activation of NF-κB and MAPK pathways as well as up-regulation of NFAT2 expression are required for osteoclastogenesis (33). The importance of NF-κB

in osteoclastogenesis is suggested by using gene deletion models. The mice lacking both NF-κB p50 and p52 or mice deficient in IKKβ exhibit severe osteopetrosis caused by failure of osteoclast formation (33, 34). Abu-Amer and colleagues (35) reported that IκB supersuppressor blocked osteoclast differentiation and activation. Moreover, the same group reported that the dominant-negative IκB protein, which lacks the NH_2-terminal phosphorylation site, lowered NF-κB activation and reduced recruitment of osteoclasts to bone erosion (36). Furthermore, IKK inhibitory peptide can suppress osteoclastogenesis and bone loss in a mouse model of arthritis (31). Thus, it is reasonable to suggest that zerumbone suppresses osteoclastogenesis through inhibition of NF-κB activation.

Malignant tumors with the skeleton as the primary site as well as metastatic bone lesions are considered a major health problem, affecting over 350,000 patients in the United States annually. Among them, 70% to 95% of patients with multiple myeloma and up to 75% of patients with advanced breast cancer or prostate cancer develop bone metastasis (37, 38). Osteoclast-mediated bone destruction is a major complication in metastatic breast cancer and multiple myeloma. In the present study, we showed that zerumbone inhibited the osteoclastogenesis induced by breast cancer and by multiple myeloma cells. Both breast cancer and multiple myeloma cells are known to express RANKL (27, 39) and to exhibit constitutive NF-κB activation (40, 41), thus implicating them in the induction of osteoclastogenesis via the expression of RANKL. We also found that breast cancer–induced bone loss in mice could be inhibited by zerumbone. Consequently, our results suggest that zerumbone could be used in the treatment of cancer-induced bone lesions. Bisphosphonate drugs (BP), potent inhibitors of osteoclast formation and activity, are the current standard of care and are most widely used drugs for treatment of cancer-induced osteolytic diseases. Their efficacy in abating pain and prolonging time to significant skeletal complications has been shown in the treatment of breast cancer–induced bone diseases (42). However, there is increasing recognition of the increased risk

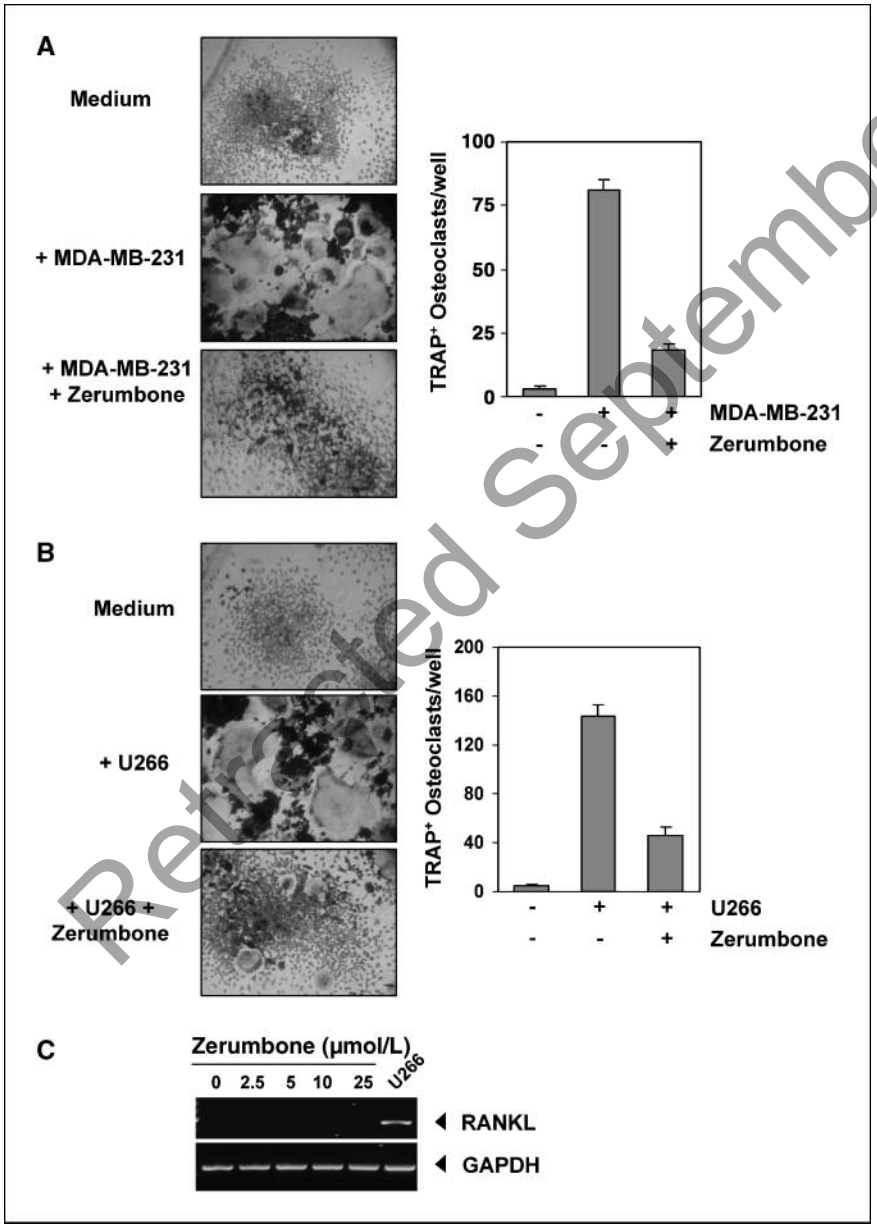

Figure 5. Zerumbone inhibits osteoclastogenesis induced by tumor cells. RAW 264.7 cells (5×10^3) were incubated in the presence of MDA-MB-231 cells (1×10^3; *A*) or U266 cells (1×10^3; *B*) for 24 h, then exposed to zerumbone (2 μmol/L) for 5 d, and finally stained for TRAP expression. Multinucleated osteoclasts (i.e., those containing three nuclei) in cocultures were counted. *C,* MDA-MB-231 cells (0.5×10^6) were incubated with indicated concentration of zerumbone for 24 h and isolated total RNA and examined for expression of RANKL using RT-PCR. U266 cells were used as a positive control for RANKL expression. GAPDH was used as an internal control to show equal RNA loading.

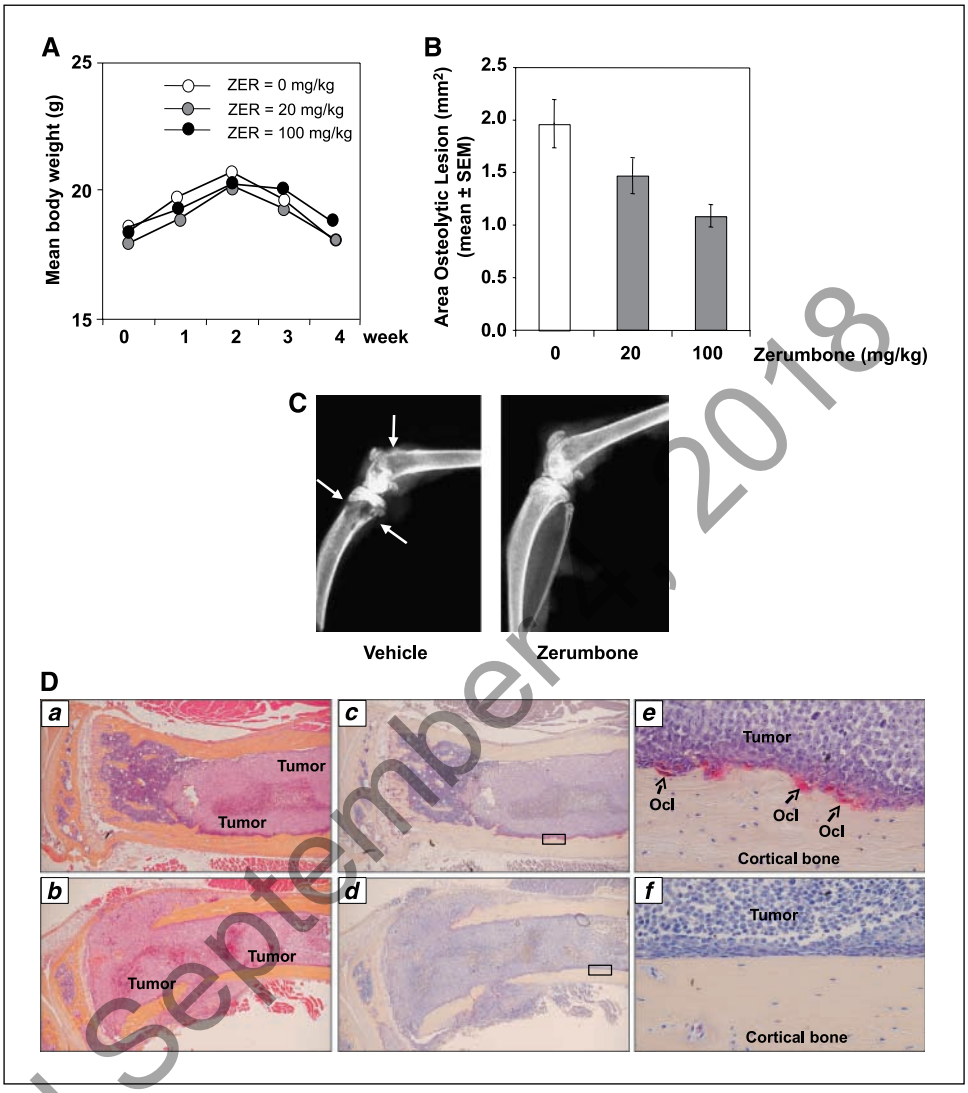

Figure 6. Zerumbone decreases breast cancer (MDA-MB-231)–induced bone loss in mice. Histograms showing the area of osteolytic lesions (*A*) and body weight (*B*) in MDA-MB-231 human breast cancer cell–bearing mice without and with zerumbone treatment (20 or 100 mg per mouse per three times in week for 28 d). Lesions were quantified by computerized image analysis from radiographs taken at sacrifice. *C,* representative radiographs from mice treated with vehicle or zerumbone (100 mg/kg) for 28 d. Note osteolytic lesions in the metaphyseal regions (represented by the marked radiolucency) and the destruction of cortices (*arrows*) in the bones from tumor-bearing mouse treated with vehicle. *D,* representative histology of tibiae of mice inoculated with human breast cancer cells indicating presence of tumor in bone (*a*) and zerumbone-treated groups (*b*). Magnification, ×4. *c* and *d,* respective serial sections stained for TRAP activity. *e* and *f,* higher magnification of tumor-bone interface delineated by the rectangles in *c* and *d*, respectively. Magnification, ×40.

of severe osteonecrosis of the jaw in cancer patients receiving BPs (43–45) with devastating consequences for affected patients (46). Thus, it is therefore prudent to develop other antiresorptive strategies to combat lytic bone lesions in patients with metastatic cancer, including breast cancer metastases. At present, a fully humanized monoclonal neutralizing antibody to RANKL, denosumab (Amgen), is ongoing in clinical trials with multiple myeloma and breast cancer and recent data suggest that it is efficacious (47).

Zerumbone is derived from a tropical ginger and thus should have minimum toxicity, as it is used routinely for traditional medicine. It could be safely used in treatment of secondary bone lesions associated with various cancers (31, 48, 49), including breast cancer, and those associated with other diseases, such as osteoporosis, Paget's disease, and rheumatoid arthritis. Zerumbone suppresses osteoclast formation *in vitro* in a RANKL-dependent manner as shown in this article. We also found that this sesquiterpene is remarkably well tolerated with no toxicity effects on systemic administration to mice at 100 mg/kg daily for 4 weeks. In comparison with BPs or denosumab, ginger is very inexpensive and thus likely to have a superior cost-benefit ratio. Because humans consume large amounts of ginger regularly in certain parts of the world with no untoward effects, these properties of zerumbone suggest potential utility of the compound, at least as adjunct therapy, in breast cancer patients. However, there are currently no preclinical data to inform well-designed clinical trials and observational studies that will be needed to determine short- and long-term effects of zerumbone and to guide clinicians and patient on its use during breast cancer treatment. The data reported in this article thus provide rationale for extensive preclinical studies on zerumbone in breast cancer.

Disclosure of Potential Conflicts of Interest

No potential conflicts of interest were disclosed.

Acknowledgments

Received 8/22/2008; revised 11/6/2008; accepted 12/5/2008; published OnlineFirst 02/03/2009.

Grant support: Clayton Foundation for Research (B.B. Aggarwal) and NIH/National Cancer Institute grants 1PO1-CA1248701-A2 (B.B. Aggarwal) and KO1CA104180 (B.O. Oyajobi). B.B. Aggarwal is the Ransom Horne, Jr., Professor of Cancer Research.

The costs of publication of this article were defrayed in part by the payment of page charges. This article must therefore be hereby marked *advertisement* in accordance with 18 U.S.C. Section 1734 solely to indicate this fact.

We thank Walter Pagel for editorial review of this manuscript and Dr. Bryant Darnay for providing the RANKL protein.

References

1. Teitelbaum SL, Ross FP. Genetic regulation of osteoclast development and function. Nat Rev Genet 2003;4:638–49.
2. Boyle WJ, Simonet WS, Lacey DL. Osteoclast differentiation and activation. Nature 2003;423:337–42.
3. Aggarwal BB. Signalling pathways of the TNF superfamily: a double-edged sword. Nat Rev Immunol 2003;3:745–56.
4. Nakashima T, Wada T, Penninger JM. RANKL and RANK as novel therapeutic targets for arthritis. Curr Opin Rheumatol 2003;15:280–7.
5. Romas E, Sims NA, Hards DK, et al. Osteoprotegerin reduces osteoclast numbers and prevents bone erosion in collagen-induced arthritis. Am J Pathol 2002;161:1419–27.
6. Kong YY, Yoshida H, Sarosi I, et al. OPGL is a key regulator of osteoclastogenesis, lymphocyte development and lymph-node organogenesis. Nature 1999;397:315–23.
7. Simonet WS, Lacey DL, Dunstan CR, et al. Osteoprotegerin: a novel secreted protein involved in the regulation of bone density. Cell 1997;89:309–19.
8. Roodman GD. Mechanisms of bone metastasis. N Engl J Med 2004;350:1655–64.
9. Mundy GR. Metastasis to bone: causes, consequences and therapeutic opportunities. Nat Rev Cancer 2002;2:584–93.
10. Ritchlin CT, Haas-Smith SA, Li P, Hicks DG, Schwarz EM. Mechanisms of TNF-α- and RANKL-mediated osteoclastogenesis and bone resorption in psoriatic arthritis. J Clin Invest 2003;111:821–31.
11. Assuma R, Oates T, Cochran D, Amar S, Graves DT. IL-1 and TNF antagonists inhibit the inflammatory response and bone loss in experimental periodontitis. J Immunol 1998;160:403–9.
12. Berenson JR. Advances in the biology and treatment of myeloma bone disease. Semin Oncol 2002;29:11–6.
13. Tanaka T, Shimizu M, Kohno H, et al. Chemoprevention of azoxymethane-induced rat aberrant crypt foci by dietary zerumbone isolated from *Zingiber zerumbet*. Life Sci 2001;69:1935–45.
14. Murakami A, Hayashi R, Tanaka T, Kwon KH, Ohigashi H, Safitri R. Suppression of dextran sodium sulfate-induced colitis in mice by zerumbone, a subtropical ginger sesquiterpene, and nimesulide: separately and in combination. Biochem Pharmacol 2003;66:1253–61.
15. Murakami A, Tanaka T, Lee JY, et al. Zerumbone, a sesquiterpene in subtropical ginger, suppresses skin tumor initiation and promotion stages in ICR mice. Int J Cancer 2004;110:481–90.
16. Huang GC, Chien TY, Chen LG, Wang CC. Antitumor effects of zerumbone from *Zingiber zerumbet* in P-388D1 cells *in vitro* and *in vivo*. Planta Med 2005;71:219–24.
17. Szabolcs A, Tiszlavicz L, Kaszaki J, et al. Zerumbone exerts a beneficial effect on inflammatory parameters of cholecystokinin octapeptide-induced experimental pancreatitis but fails to improve histology. Pancreas 2007;35:249–55.
18. Takada Y, Murakami A, Aggarwal BB. Zerumbone abolishes NF-κB and IκBα kinase activation leading to suppression of antiapoptotic and metastatic gene expression, upregulation of apoptosis, and downregulation of invasion. Oncogene 2005;24:6957–69.
19. Murakami A, Takahashi M, Jiwajinda S, Koshimizu K, Ohigashi H. Identification of zerumbone in *Zingiber zerumbet* Smith as a potent inhibitor of 12-*O*-tetradecanoylphorbol-13-acetate-induced Epstein-Barr virus activation. Biosci Biotechnol Biochem 1999;63:1811–2.
20. Hsu H, Lacey DL, Dunstan CR, et al. Tumor necrosis factor receptor family member RANK mediates osteoclast differentiation and activation induced by osteoprotegerin ligand. Proc Natl Acad Sci U S A 1999;96:3540–5.
21. Wei S, Teitelbaum SL, Wang MW, Ross FP. Receptor activator of nuclear factor-κB ligand activates nuclear factor-κB in osteoclast precursors. Endocrinology 2001;142:1290–5.
22. Sung B, Pandey MK, Aggarwal BB. Fisetin, an inhibitor of cyclin-dependent kinase 6, down-regulates nuclear factor-κB-regulated cell proliferation, antiapoptotic and metastatic gene products through the suppression of TAK-1 and receptor-interacting protein-regulated IκBα kinase activation. Mol Pharmacol 2007;71:1703–14.
23. Oyajobi BO, Anderson DM, Traianedes K, Williams PJ, Yoneda T, Mundy GR. Therapeutic efficacy of a soluble receptor activator of nuclear factor κB-IgG Fc fusion protein in suppressing bone resorption and hypercalcemia in a model of humoral hypercalcemia of malignancy. Cancer Res 2001;61:2572–8.
24. Kobayashi Y, Mizoguchi T, Take I, Kurihara S, Udagawa N, Takahashi N. Prostaglandin E2 enhances osteoclastic differentiation of precursor cells through protein kinase A-dependent phosphorylation of TAK1. J Biol Chem 2005;280:11395–403.
25. Ghosh S, Karin M. Missing pieces in the NF-κB puzzle. Cell 2002;109 Suppl:S81–96.
26. Chikatsu N, Takeuchi Y, Tamura Y, et al. Interactions between cancer and bone marrow cells induce osteoclast differentiation factor expression and osteoclast-like cell formation *in vitro*. Biochem Biophys Res Commun 2000;267:632–7.
27. Lai FP, Cole-Sinclair M, Cheng WJ, et al. Myeloma cells can directly contribute to the pool of RANKL in bone bypassing the classic stromal and osteoblast pathway of osteoclast stimulation. Br J Haematol 2004;126:192–201.
28. Park BK, Zhang H, Zeng Q, et al. NF-κB in breast cancer cells promotes osteolytic bone metastasis by inducing osteoclastogenesis via GM-CSF. Nat Med 2007;13:62–9.
29. Uhlik M, Good L, Xiao G, et al. NF-κB-inducing kinase and IκB kinase participate in human T-cell leukemia virus I Tax-mediated NF-κB activation. J Biol Chem 1998;273:21132–6.
30. Novack DV, Yin L, Hagen-Stapleton A, et al. The IκB function of NF-κB2 p100 controls stimulated osteoclastogenesis. J Exp Med 2003;198:771–81.
31. Dai S, Hirayama T, Abbas S, Abu-Amer Y. The IκB kinase (IKK) inhibitor, NEMO-binding domain peptide, blocks osteoclastogenesis and bone erosion in inflammatory arthritis. J Biol Chem 2004;279:37219–22.
32. Aggarwal BB. Nuclear factor-κB: the enemy within. Cancer Cell 2004;6:203–8.
33. Zheng H, Yu X, Collin-Osdoby P, Osdoby P. RANKL stimulates inducible nitric-oxide synthase expression and nitric oxide production in developing osteoclasts. An autocrine negative feedback mechanism triggered by RANKL-induced interferon-β via NF-κB that restrains osteoclastogenesis and bone resorption. J Biol Chem 2006;281:15809–20.
34. Franzoso G, Carlson L, Xing L, et al. Requirement for NF-κB in osteoclast and B-cell development. Genes Dev 1997;11:3482–96.
35. Abu-Amer Y, Dowdy SF, Ross FP, Clohisy JC, Teitelbaum SL. TAT fusion proteins containing tyrosine 42-deleted IκBα arrest osteoclastogenesis. J Biol Chem 2001;276:30499–503.
36. Clohisy JC, Roy BC, Biondo C, et al. Direct inhibition of NF-κB blocks bone erosion associated with inflammatory arthritis. J Immunol 2003;171:5547–53.
37. Carlin BI, Andriole GL. The natural history, skeletal complications, and management of bone metastases in patients with prostate carcinoma. Cancer 2000;88:2989–94.
38. Coleman RE. Metastatic bone disease: clinical features, pathophysiology and treatment strategies. Cancer Treat Rev 2001;27:165–76.
39. Bhatia P, Sanders MM, Hansen MF. Expression of receptor activator of nuclear factor-κB is inversely correlated with metastatic phenotype in breast carcinoma. Clin Cancer Res 2005;11:162–5.
40. Bharti AC, Shishodia S, Reuben JM, et al. Nuclear factor-κB and STAT3 are constitutively active in CD138$^+$ cells derived from multiple myeloma patients, and suppression of these transcription factors leads to apoptosis. Blood 2004;103:3175–84.
41. Biswas DK, Shi Q, Baily S, et al. NF-κB activation in human breast cancer specimens and its role in cell proliferation and apoptosis. Proc Natl Acad Sci U S A 2004;101:10137–42.
42. Lipton A. Biochemical bone markers in breast cancer. Cancer Treat Rev 2006;32 Suppl 1:20–2.
43. Cartsos VM, Zhu S, Zavras AI. Bisphosphonate use and the risk of adverse jaw outcomes: a medical claims study of 714,217 people. J Am Dent Assoc 2008;139:23–30.
44. Mariotti A. Bisphosphonates and osteonecrosis of the jaws. J Dent Educ 2008;72:919–29.
45. Hoff AO, Toth BB, Altundag K, et al. Frequency and risk factors associated with osteonecrosis of the jaw in cancer patients treated with intravenous bisphosphonates. J Bone Miner Res 2008;23:826–36.
46. Gevorgyan A, Enepekides DJ. Bisphosphonate-induced necrosis of the jaws: a reconstructive nightmare. Curr Opin Otolaryngol Head Neck Surg 2008;16:325–30.
47. Body JJ, Facon T, Coleman RE, et al. A study of the biological receptor activator of nuclear factor-κB ligand inhibitor, denosumab, in patients with multiple myeloma or bone metastases from breast cancer. Clin Cancer Res 2006;12:1221–8.
48. Hunt NC, Fujikawa Y, Sabokbar A, Itonaga I, Harris A, Athanasou NA. Cellular mechanisms of bone resorption in breast carcinoma. Br J Cancer 2001;85:78–84.
49. Tada T, Jimi E, Okamoto M, Ozeki S, Okabe K. Oral squamous cell carcinoma cells induce osteoclast differentiation by suppression of osteoprotegerin expression in osteoblasts. Int J Cancer 2005;116:253–62.